Stochastic inversion of 2D magnetotelluric data using pixel-based parameterization

Jinsong Chen, Lawrence Berkeley National Laboratory, G. Michael Hoversten, Chevron Energy Technology Company, and Gregg Nordquist, Chevron Geothermal Services Company*

Summary

We develop a Bayesian model to invert 2D magnetotelluric (MT) data using a pixel-based parameterization, and apply it to an active geothermal field. Although this parameterization is more flexible in representing subsurface resistivity structure than sharp boundary models, it may cause problems for Markov chain Monte Carlo (MCMC) based Bayesian methods because it significantly increases the total number of unknowns, most of which are spatially correlated. The key to success for stochastic approaches is to employ a suitable prior model to represent the spatial dependence and to develop efficient sampling strategies for exploring the joint posterior distribution. In this study, we use a Gaussian Markov random field with an unknown controlling parameter to describe the spatial dependence of the resistivity and use gradient-based algorithms to draw MCMC samples. To shorten the burn-in time, we run multiple chains from the local optimal solution found by Occam inversion methods. The case study results show the developed stochastic method and the sampling strategies are effective for 2D MT inversion. Compared to deterministic inversion methods, such as 2D Occam inversion or 3D Gauss-Newton methods, the stochastic method provides significantly more uncertainty information on the features of interest.

Introduction

Current approaches for inverting 2D or 3D electromagnetic (EM) data are primarily Gauss-Newton based deterministic methods (e.g., Newman and Alumbaugh, 2000; Abubakar et al., 2008) using pixel-based parameterizations. These types of methods have two major advantages: (1) using pixel-based parameterizations so that they can handle a wide range of inverse problems without making assumptions on the targets of interest, and (2) using Gauss-Newton iteration methods to find optimal solutions so that they can solve a complex inverse problem with tens of millions of unknowns in tens to hundreds of iterations. However, the optimal solutions found are often local and depend on the choice of initial values; additionally, they provide very limited information on uncertainty of the estimated parameters.

Stochastic inversion methods, specifically Bayesian models with Markov chain Monte Carlo (MCMC) sampling methods (Gilks et al, 1996), have been recognized as a powerful approach for solving geophysical inverse problems (Tarantola, 2005). As demonstrated by Chen et al. (2008), stochastic inversion methods can provide extensive uncertainty information about unknown parameters; inversion results are almost independent of initial values and therefore global and robust. Because stochastic methods often need to run forward models tens of thousands of times and computing time typically is proportional to the number of unknowns, current applications are limited to problems where fast forward models are available, such as inversion of 1D seismic data (Gunning and Glinsky, 2004) and joint inversion of 1D seismic and EM data (Chen et al., 2007), or problems with less numbers of unknowns, such as stochastic inversion of 2D MT data using sharp boundary parameterizations (Chen et al., 2012).

In this study, we take advantage of both Gauss-Newton and Bayesian approaches to develop a stochastic inversion method to invert 2D MT data for geothermal applications. We use a pixel-based parameterization in the model so that we can estimate any shape of targets. We use Gaussian Markov random fields to explicitly model the spatial variability of unknown electrical resistivity, rather than using regularization schemes to enforce smoothing in Gauss-Newton based methods. We use a gradient-based MCMC sampling technique developed by Roberts and Tweedie (1996). We use the parallel, adaptive finite-element algorithm developed by Key and Ovall (2011) to forward simulate MT responses.

Method

<u>Parameterization and Bayesian model</u>

We divide a 2D cross section into two regions, one being the region of interest and the other being the area surrounding the region. We divide the focus region into $m \times n$ quadrilateral pixels (i.e., m rows and n columns), and assume electrical resistivity at each pixel is unknown. Let r_{ij} be the unknown resistivity in the pixel at the i-th row and j-th column, where $i = 1, 2, \cdots, m$, and $j = 1, 2, \cdots, n$. We can use different parameterizations, such as triangulation to divide the background region into numbers of triangular elements and consider resistivity at those elements as unknowns. In the current study, we just extend laterally the pixels adjacent to the focus region to the two far bounds, and consider the zone between the focus area and the far vertical bound as one big block and let its resistivity be r_0.

We introduce two additional unknown variables to address the spatial variability of resistivity and the errors in the forward simulation of MT responses. Let θ be the parameter

determining the spatial dependence and τ be the parameter associated with the integrated errors in MT measurements and in the forward modeling. The detailed meaning of the two variables will be given later in the text.

The data used for the inversion are apparent resistivity and phase defined by Smith and Booker (1991) for TE and TM mode complex impedance. Let vector $\mathbf{y}$ represent all the MT data. Let vector $\mathbf{x}$ represent all the unknown logarithmic resistivity, arranged first by columns and then by rows. Thus, we have the following Bayesian model

$$f(\mathbf{x},\tau,\theta \mid \mathbf{y}) \propto f(\mathbf{y} \mid \mathbf{x},\tau) f(\mathbf{x} \mid \theta) f(\theta) f(\tau) . \qquad (1)$$

Equation 1 defines a joint posterior probability distribution of all unknown parameters, which is known up to a normalizing constant. The first term on the right side of the equation is the likelihood function of 2D MT data, which is the linkage between the unknown resistivity and the MT data. The other terms are determined by the information other than the MT data, such as prior beliefs on the spatial dependence and their associated parameters.

Likelihood model

The likelihood function in equation 1 plays a central role in the Bayesian inversion; it is a probabilistic description of the integrated discrepancies between the measured MT data and the forward modeling results. Since we typically have some information on measurement errors (referred to as 'nominated errors'), we assume that the integrated discrepancies are proportional to the measurement errors. Let τ be the ratio of the variance of the nominated errors to the variance of the integrated differences. We jointly estimate this ratio in the inversion. By assuming the nominated errors are independent and have the Gaussian distribution with zero mean and a given standard deviation, we obtain the following likelihood model

$$f(\mathbf{y} \mid \mathbf{x},\tau) = \prod_{i=1}^{N} \frac{1}{\sigma_i^{ref}\sqrt{2\pi}} \tau^{1/2} \exp\left\{ -\frac{\tau}{2} \left(\frac{y_i^{obs} - y_i^{calc}}{\sigma_i^{ref}} \right)^2 \right\}. \qquad (2)$$

In equation 2, N is the total number of data points, σ_i^{ref} is the standard deviation of the nominated errors, and y_i^{obs} and y_i^{calc} are the observed and calculated MT responses.

Prior model for spatial dependence

We use a Gaussian Markov random field as the prior model to describe the spatial dependence of resistivity. As demonstrated by Lee et al. (2002), Markov random fields based spatial priors have several advantages over variogram-based or Gaussian spatial process priors. For example, they provide multiple scale information and need less number of control parameters. Let θ be the precision parameter controlling the spatial scale of resistivity and let matrix $\mathbf{W}$ be the precision matrix controlling the spatial dependence. We have the following spatial prior model

$$f(\mathbf{x} \mid \theta) \propto \theta^{N/2} \left|\mathbf{W}\right|^{1/2} \exp\left\{ -\frac{1}{2}\theta \mathbf{x}^T \mathbf{W} \mathbf{x} \right\}. \qquad (3)$$

In equation 3, '$|\cdot|$' represents the matrix determinant, and T represents the transpose of vectors. To complete the specification of priors in equation 1, we assume both θ and τ have Gamma distributions. This is a common and convenient assumption for precision parameters.

Gradient-based MCMC sampling methods

The success of stochastic inversion methods depends on the efficiencies of MCMC sampling methods. Since our MT forward model can calculate the gradients of unknowns efficiently, we use gradient-based algorithms to draw samples of resistivity. This method has been shown by Roberts and Rosenthal (2001) to have a wide range of optimal acceptance rates and the cubic root time scaling in terms of the number of unknowns.

Case Study

We applied the developed stochastic method to a synthetic model similar to the one given by Chen et al. (2012) and to an operating geothermal field. Given the limited space, we only report in the following the results of the field case study.

MT survey and data

The MT data collected over the geothermal field have provided important constraints on the interpretations of the areal extent and location of the field during the exploration and development of the field. More than 90 MT stations have been deployed at the site over time. In this study, we use the MT data at the sites on or near the profile starting from Station 431 and ending at Station 116 as shown in Figure 1. This profile includes 12 sites and is approximately perpendicular to the observed geo-electric strike direction. At each site, we have apparent resistivity and phases with frequencies from 0.01 Hz to 100 Hz for both TE and TM modes.

2D Occam deterministic inversion

We use pixel-based parameterizations in this study, which is different from the sharp-boundary parameterization used in Chen et al. (2012). The focus region spans laterally over 100 km and vertically from the ground surface up to 15 km downwards. We divide the cross section into 28×22 quadrilateral pixels. The lateral discretization size varies based on the ground surface geometry; the vertical discretization size increases from 30 m at the shallow layers to 1000 m at the deep layers. We set the lower and upper bounds as 0.001 and 1000 ohm-m for resistivity at all the pixels.

Pixel-based stochastic inversion of 2D MT data

We first use the 2D Occam codes developed by Key (2012) to invert the MT data by starting from the 30 ohm-m half-space and enforcing an anisotropic spatial smoothing of 3:1 (horizontal vs. vertical). The algorithm is converged to the root-mean-square errors (RMS) of 1.80 after 15 iterations; the resultant 2D image is shown in Figure 2. As a comparison, we also show the 3D deterministic inversion results from Chen et al. (2012) in Figure 3. The 3D inversion uses the Gauss-Newton method developed by Newman et al. (2008) to fit the MT data collected from 85 stations to the RMS of 1.40 by starting from a half-space with the resistivity of 10 ohm-m. Although the Occam inversion only uses the TM mode data along the 2D profile, overall they have similar patterns along the lateral and in the vertical directions, such as the persistence in the near surface layers, the clay cap layer, and the deep resistive layers.

2D stochastic inversion

We use the same parameterization as the Occam method to invert the same TM mode data using our pixel-based stochastic method. We run four chains for 40,000 iterations and each starts from the optimal model found by the Occam inversion but using different random seeds. For the MCMC based Bayesian model, we can start from any initial value, for instance, the half-space model or a model formed from random values. The initial values do not affect inversion results after convergence but affect the burn-in time to reach the convergence. Figure 4 shows the RMS of four chains as a function of iterations after a thinning of two. We use the second half of three chains (i.e., black, red, and blue) for the subsequent analysis based on the convergence diagnostics of Gelman and Rubin (1992). The resultant RMS is significantly less than the one from the Occam inversion (RMS=1.80); it is random and has the mean of 1.349 and the standard deviation of 0.088. This suggests the model found by the Occam method just is a local optimal solution.

Figure 5 shows the median of the estimated resistivity. Compared to Figures 2 and 3, they are very similar visually and all delineate the conductive clay cap. However, considerable discrepancies exist, especially in the deeper layers. For example, on the area within the dashed rectangle, the high resistivity region is on the right side in Figure 2, on the left side in Figures 3, and on both sides in Figure 5.

Quantification of uncertainty

One of the main advantages of stochastic inversion methods is that they provide extensive uncertainty information on the estimated parameters. Unlike the 2D Occam or 3D Gauss-Newton inversion methods, which provide only one optimal solution, the stochastic method provides 30,000 models that fit the data almost equally well (see Figure 4). Using those models, we can estimate the probability distribution of any quantity that we are interested in. For geothermal applications, the electrical conductivity and its distribution are often used to interpret the clay cap; thus, they can be used to estimate the bounds of a potential reservoir (Cumming, 2009). The uncertainty information associated with the clay cap can be used to derive the value of information for risk-based decision making (Trainor-Guitton, 2014). In the following, we quantify uncertainties in the properties associated with the clay cap. For each model (or realization), we first calculate conductivities (i.e., the reciprocal of resistivity) and use 75% quantile of the conductivities as the cutoff to identify the locations of upper and lower interfaces of the clay cap. This leads to the cutoff value around 0.25 S/m. We found the relative cutoff is more reliable than an absolute value because some models may overall have smaller values than others. The 75% is arbitrary and we can certainly use other quantiles.

Figure 6 shows the estimated probability density of the conductance at location x=0.83 based on the 30,000 MCMC samples, where the red and blue vertical line segments correspond to the results from the 2D Occam and 3D inversion. According to the estimated posterior probability distribution, the values derived from the 2D Occam and from the 3D inversion are both plausible. Figure 7 shows the 95% predictive intervals of the clay cap conductance, the thickness, the locations of the upper interface, and the locations of the lower interface. The red dashed lines are the lower and upper bounds of the 95% predictive intervals and the black line segments with squares are the medians. The blue and green line segments are the results from the 2D Occam and 3D Gauss-Newton inversion, respectively. As shown in the figure, the uncertainty varies laterally; fewer uncertainties occur near the center (i.e., the horizontal location of 0.5). Around the center, where data coverage is a maximum, all three methods give similar results.

Conclusions

The case study results show the developed pixel-based Bayesian model with gradient-based MCMC sampling algorithms is effective for inverting MT data. Deterministic and stochastic inversion methods complement each other and should be used together, with the former providing initial models for significantly reducing MCMC burn-in time and the latter providing the global estimates of unknown parameters and their associated uncertainty information, which is needed for resource estimation techniques.

Acknowledgments

The work is funded by Chevron Energy Technology Company. We thank Chevron for permission to publish this work. We also thank Kerry Key in the University of California at San Diego for allowing us to use his MARE2DEM codes.

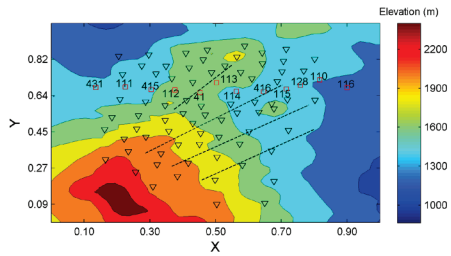

Figure 1: Locations of MT stations.

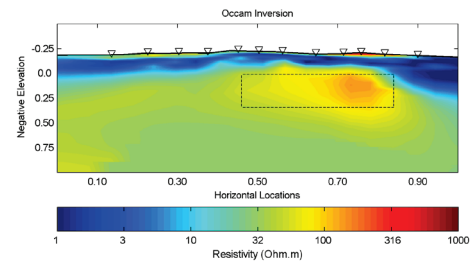

Figure 2: 2D Occam inversion results.

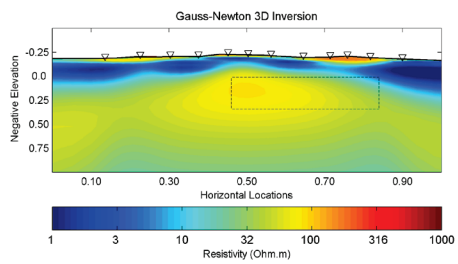

Figure 3: 3D Gauss-Newton inversion results.

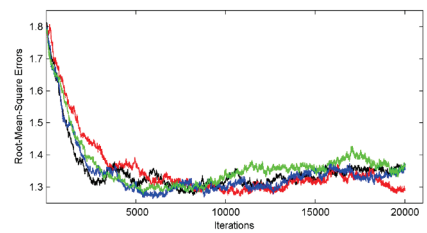

Figure 4: RMS as a function of iterations for four MCMC chains (using a thinning of two).

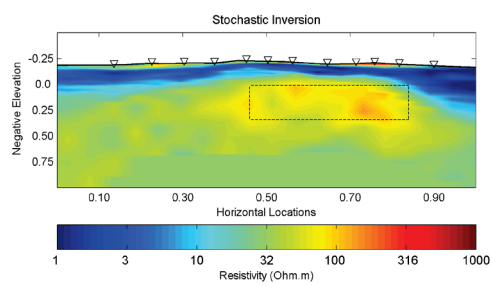

Figure 5: Stochastic inversion results.

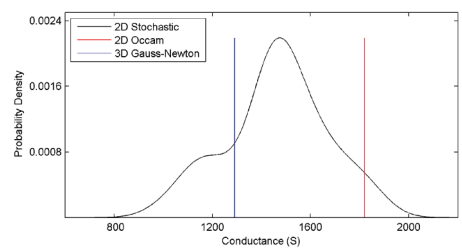

Figure 6: Estimated probability density for the clay cap conductance at the horizontal location of 0.83.

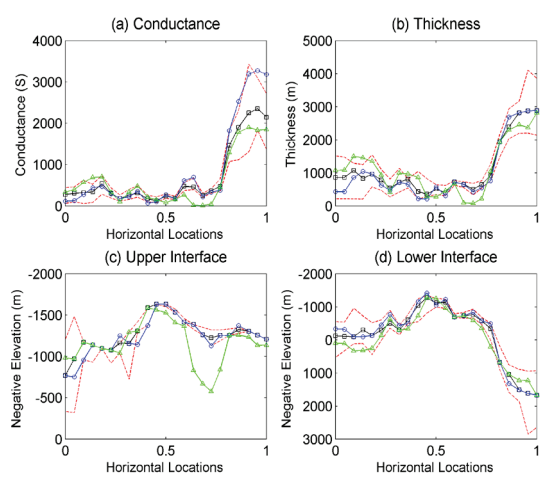

Figure 7: Comparison of the results from 2D stochastic and Occam inversion and from 3D Gauss-Newton estimation. The red dashed lines and the black line segments with squares are the 95% predictive intervals and the estimated medians from stochastic inversion. The blue line segments with circles and green line segments with triangles are the estimates from 2D Occam and 3D Gauss-Newton inversion, respectively.